Design and synthesis of water-soluble prodrugs of rifabutin for intraveneous administration

Kevin Antraygues, Mathieu Maingot, Birgit Schellhorn, Vincent Trebosc, Marc Gitzinger, Benoit Déprez, Olivier Defert, Glenn E Dale, Marilyne Bourotte, Sergio Lociuro, et al.

Design and synthesis of water-soluble prodrugs of rifabutin for intraveneous administration

Kevin Antraygues[1], Mathieu Maingot[1], Birgit Schellhorn[3], Vincent Trebosc[3], Marc Gitzinger[3], Benoit Déprez[1], Olivier Defert[2], Glenn E. Dale[3], Marilyne Bourotte[2], Sergio Lociuro[3], Nicolas Willand[1,*]

[1] Univ. Lille, Inserm, Institut Pasteur de Lille, U1177 - Drugs and Molecules for Living Systems, F-59000, Lille, France.

[2] BioVersys SAS, Lille, France.

[3] BioVersys AG, Basel, Switzerland.

*nicolas.willand@univ-lille.fr

ABSTRACT

Acinetobacter baumannii is a gram-negative bacterium causing severe hospital-acquired infections such as bloodstream infections or pneumonia. Moreover, multidrug resistant *A. baumannii* becomes prevalent in many hospitals. Consequently, the World Health Organization made this bacterium a critical priority for the research and development of new antibiotics. Rifabutin, a semisynthetic product from the rifamycin class, was recently found to be very active in nutrient-limited eukaryotic cell culture medium against various *A. baumannii* strains, including extremely drug-resistant strains, with minimal inhibitory concentrations as low as 0.008 µg/mL. Moreover, this *in vitro* potency translates into *in vivo* efficacy. Thus, rifabutin appears to be an attractive novel antibiotic against *A. baumannii*. In this work, our objective was to design and synthetize rifabutin prodrugs with increased aqueous solubility to allow intraveneous use. Synthetic methodologies were developed to selectively functionalize the hydroxyl group in position 21 and to afford 17 prodrugs. We measured the water solubility of the prodrugs, the stability in human and mouse plasma and their antimicrobial activity against *A. baumannii* after incubation in human serum. Finally, a pharmacokinetic release study of rifabutin was performed in CD1 mice with three selected prodrugs as a proof of concept.

Keywords:

Rifabutin prodrugs, A. baumannii, self-immolative linkers, antimicrobial resistance

Graphical abstract

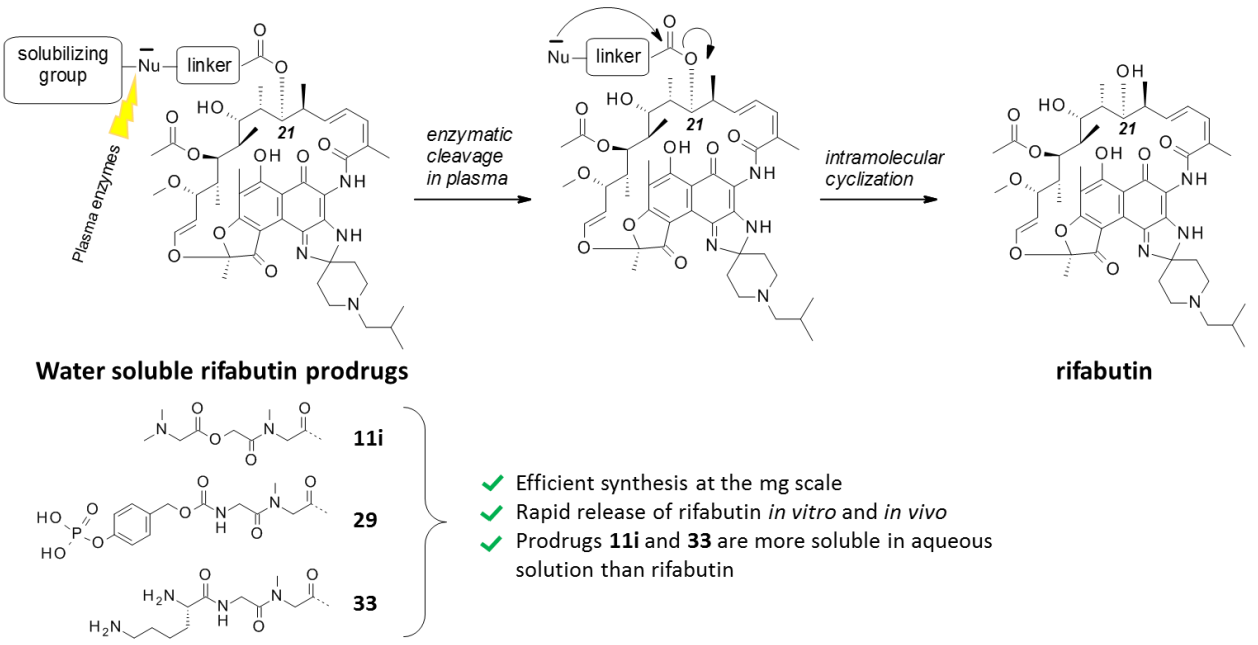

1. Introduction

Rifabutin (also known as LM 427 and Mycobutin®) is a spiro-piperidyl-rifamycin derived from rifamycin-S, belonging to the class of ansamycins. The antimicrobial activity of the rifamycins is based on their ability to penetrate the bacterial cell wall and to inhibit DNA-dependent RNA polymerase with a subsequent inhibition of transcription and protein synthesis. Rifabutin has a broad spectrum of antimicrobial activity. This includes activity against mycobacteria, a variety of Gram-positive and Gram-negative bacteria, *Chlamydia trachomatis*, and *Toxoplasma gondii*. [1] *Escherichia coli* and other Gram-negative enteric bacteria and nonfermenting Gram-negative bacilli are resistant to rifabutin at concentrations that can be readily achieved in blood. [2] It has been established that the drug's penetration through the bacteria cell wall explains the higher potency against Gram-positive compared to the Gram-negative despite the quite similar RNA polymerase inhibitory activities. [3]

Acinetobacter baumannii is a Gram-negative pathogen causing severe hospital-acquired infections such as pneumonia and sepsis, with a fatality rate between 50 and 60 %. [4] The World Health Organization categorized carbapenem resistant *A. baumannii* as a critical priority for the research and development of new antibiotics due to current limited effective therapeutic options. [5] In this context, the ReFRAME library, a collection of 12,000 compounds that have been

marketed or have reached clinical development, [6] was screened for *in vitro* activity against *A. baumannii* in nutrient-limited eukariotic cell culture medium to mimic the host environment. Rifabutin was identified as the most potent hit [7] and displayed minimal inhibitory concentrations (MICs) against *A. baumannii* strains as low as 0.008 µg/mL. Interestingly, MICs of rifampicin, similarly to all other rifamycin antibiotic tested, remained invariably high independently of the culture medium used. In studies of the mechanism of action, rifabutin was shown to be actively transported in *A. baumannii* through the TonB-dependent siderophore transporter FhuE. [7] More importantly, *in vitro* activity in iron-limited condition was shown to translate well into *in vivo* efficacy [7] and PK/PD studies revealed that whereas AUC/MIC is the primary driver for efficacy, C_{max}/MIC is an important secondary driver and may be especially important not only for efficacy but to reduce chances of resistance development. [8] Thus, to optimize rifabutin exposures (AUC) and C_{max} and to mininimize the intrinsic interpatient variability inherent to oral dosing, [9] the intrinsic low acqueous solubility of rifabutin was overcome with a new intravenous (IV) formulation (BV100) [US20210077470A1]. BV100 is currently evaluated in three clinical phase I trial studies (NCT04636983, NCT05087069, NCT05086107). [10,11,12].

Alternatively, we aimed at synthesizing prodrugs capable of rapidly regenerating rifabutin in human plasma while demonstrating improved aqueous solubility. We report here the design, the synthesis and the physicochemical and pharmacokinetic characterization of rifabutin prodrugs for intravenous use. To date, only bisphosphonate rifabutin prodrugs have been studied to target bone infections caused by *Staphyloccocus aureus* and release the parent drug at the site of infections [13,14].

Two points of attachment were considered to introduce the promoiety on the rifabutin scaffold with three different chemical bonds: the imidazoline ring through regioselective acylation using either acyl chlorides or chloroformates to yield amides and carbamates, respectively [15–18] or the hydroxyl group at the C-21 position through regioselective acylation using anhydrides to form esters. [13,14,19]

As described in Scheme 1, rifabutin prodrugs amide **1**, carbamate **2** and ester **3** were synthesized and their stability in human plasma and their MIC on *A. baumannii* were evaluated *in vitro* (Table 1).

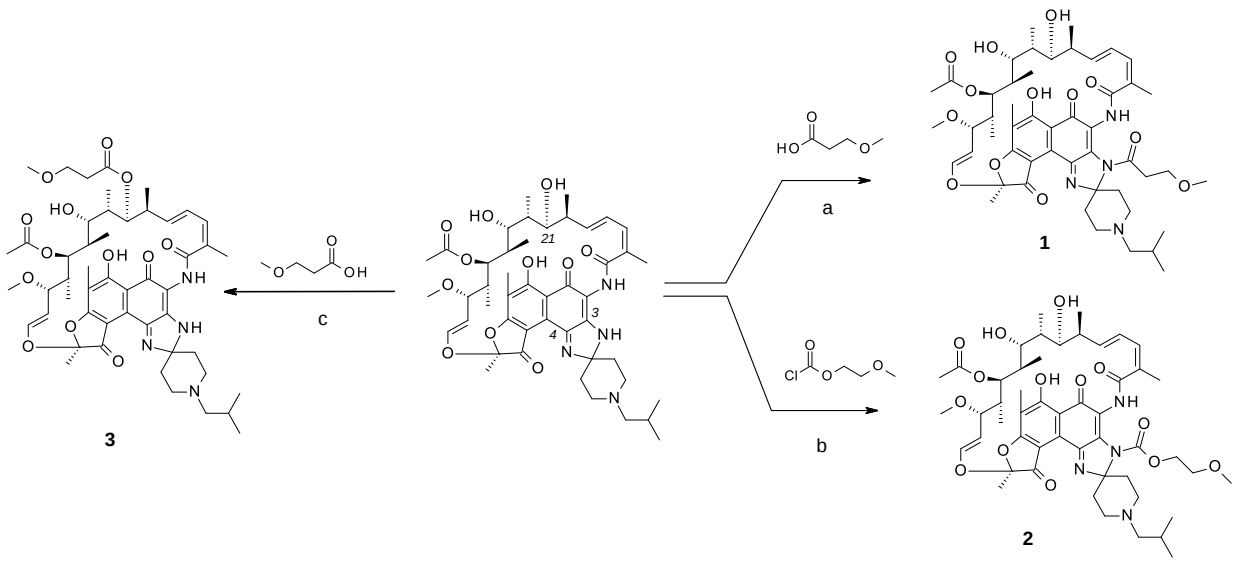

Scheme 1. Synthetic pathway for ribabutin amide (**1**), carbamate (**2**) and ester **3** prodrugs. Reagents and conditions; (a) $SOCl_2$, reflux then Et_3N, THF, 0 °C to RT, quant.; (b) 1,8-Bis(dimethylamino)naphthalene, THF, RT, 77 %; (c) DCC, CH_2Cl_2, RT then DMAP, THF, RT, 51 %.

Table 1. Stability in human plasma *and in vitro* activity against *A. baumannii* of compounds **1** to **3**.

Compound	% remaining at 6 h[a]	MIC[b] (µg/mL)
rifabutin	/	0.002
1	2 ± 0.1	N.D.
2	86 ± 1.0	0.06
3	99 ± 1.3	> 32

[a] Experiments were performed in duplicate

[b] Medium culture: RPMI + 10 % FCS

Amide **1** had quantitatively released rifabutin within 6h (Table 1). Unfortunately, this compound as well as other amide derivatives were found to be unstable under purification conditions or in the presence of water. Due to the overall poor chemical stability of this series, this functionalization was discarded. Carbamate **2** was more stable in aqueous solution but also in human plasma with a remaining percentage at 6 h of 86 %. Nevertheless, a potent bacterial growth inhibition was observed, with a MIC of 0.06 µg/mL, which is in accordance with published *N*-substituted derivatives that maintained potency against *S. aureus* and *Mycobacterium tuberculosis*. [14,15] Therefore, carbamate **2** could not be considered as a true prodrug. Finally, ester **3** was also stable

in plasma (99 % remaining at 6 h) and did not show any *A. baumannii* growth inhibition at the tested concentrations (MIC > 32 µg/mL). Indeed, the hydroxyl group at the C-21 position is mandatory for the interaction with bacterial RNA-polymerase and therefore for the growth inhibition activity. [20] As enzymatic conversion of prodrugs is dependent on accessibility of the scissile bond to the enzyme, we decided to pursue modifications of the C-21 position with spacers between the scissile bond and the rifabutin core. To improve the hydrolysis of these derivatives in plasma, we employed intramolecular spontaneous cyclization strategies and self-immolative linkers (Fig 1). The hydroxyl group at C-21 was connected through an ester bound to a linker, which carries a nucleophilic atom (nitrogen or oxygen). Nucleophilicity of the latter is masked by an amide, an ester or a phosphate bound linked to the solubilizing group. Upon enzymatic deacylation of the nitrogen, spontaneous intramolecular cyclisation could result in rifabutin release (**Type A** rifabutin prodrugs, Fig 1). We also considered the use of self-immolative linkers such as *p*-hydroxybenzylalcohol (PHBA) or “trimethyl lock” (TML) systems (**Type B** rifabutin prodrugs, Fig 1). [21–23]

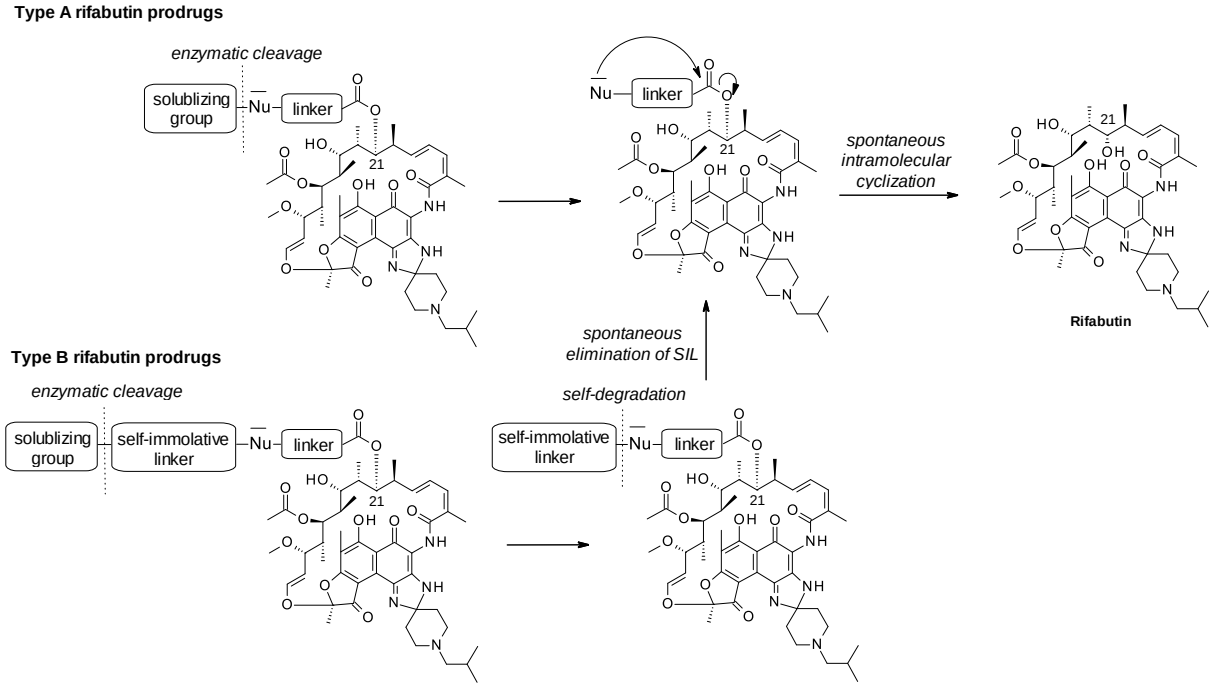

Fig 1. General scheme of intramolecular cyclization strategy from type A and B prodrugs (respectively without or with a self-immolative linker (SIL)). Nu = NH or O.

2. Chemistry

2.1. Synthesis of type A prodrugs

Type A rifabutin prodrugs were synthesized by coupling moieties carrying the solubilizing group through an amide bound to Gly-rifabutin (intermediate **6**, Fig 2) or Sar-rifabutin (intermediate **7**, Fig 2). The first strategy to increase water-solubility was to use L-amino acids as prodrug moieties. The second strategy was to incorporate a phopshate group via a glycolyl linker, and the third strategy was to introduce a dimethylglycine via the same linker. Three different series of type A prodrugs, named according to the scissile bond, were obtained: amide, phosphate and ester (Fig **2**).

For all these compounds, the spontaneous intramolecular cyclization after cleavage would also lead to the release of diketopiperazine (piperazine-2,5-dione or 1-methyl-piperazine-2,5-dione) or diketomorpholine (4-methylmorpholine-2,5-dione) in addition to rifabutin. Moieties leading to these cyclic metabolites through intramolecular cyclization have been widely reported in the literature for the preparation of prodrugs and have not been described as causing side-effects. [24–27]

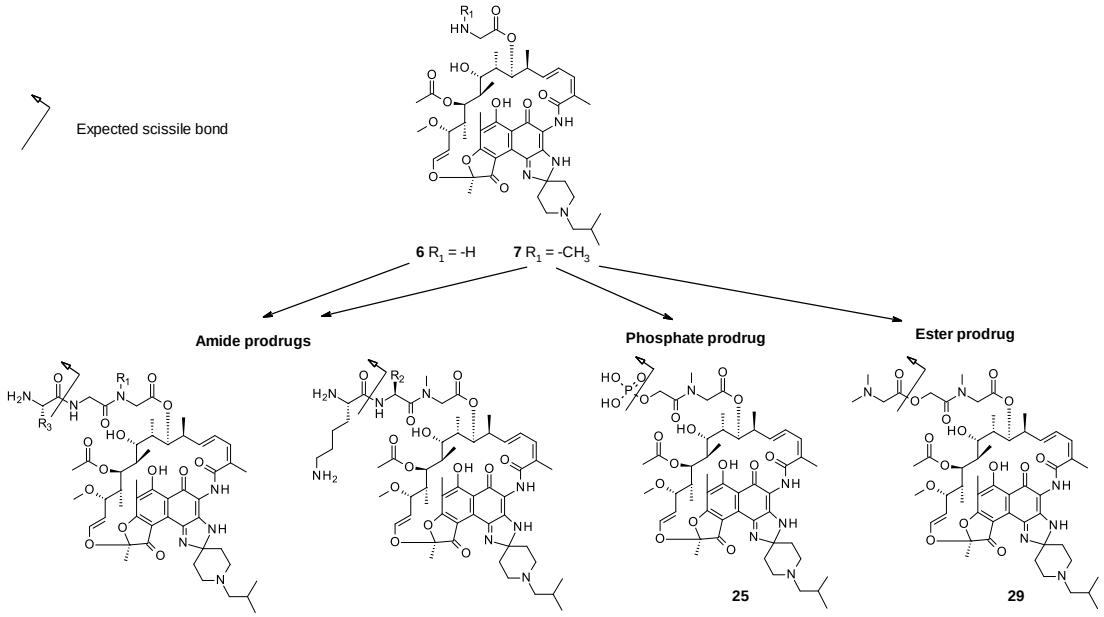

R_1 = -H (glycyl derivative)
11a R_3 = $-CH_2CH_2CH_2CH_2-NH_2$ (AA = L-Lys)

21a R_2 = $-CH_2CH_2CH_2CH_2NH_2$ (AA = L-Lys)
21b R_2 = $-CH_2CH_2CH_2NH$- (AA = L-Pro)

R_1 = $-CH_3$ (sarcosyl derivatives)
11b R_3 = -H (AA = Gly)
11c R_3 = $-CH_2OH$ (AA = L-Ser)
11d R_3 = $-CH(CH_3)OH$ (AA = L-Thr)
11e R_3 = $-CH_2CONH_2$ (AA = L-Asn)
11f R_3 = $-CH_2CH_2CONH_2$ (AA = L-Gln)
11g R_3 = $-CH_2$-Im (AA = L-His)
11h R_3 = $-CH_2CH_2CH_2-NH_2$ (AA = L-Orn)
11i R_3 = $-CH_2CH_2CH_2CH_2-NH_2$ (AA = L-Lys)
17a R_3 = $-CH_2COOH$ (AA = L-Asp)
17b R_3 = $-CH_2CH_2COOH$ (AA = L-Glu)

Fig 2. Description of the targeted type A amide, phosphate and ester prodrugs obtained from Gly-RBT (**6**) or Sar-RBT (**7**).

2.1.1. Synthesis of type A rifabutin amide prodrugs

The synthesis of intermediates **6** and **7** was achieved through the regioselective acylation of rifabutin at position 21 with either Fmoc-glycine or Fmoc-sarcosine (Scheme 2) by adapting a protocol described by Dietrich *et al*. [13,14] The structure of compound **5** was confirmed by 1D and 2D NMR (Fig. S1). The Fmoc protecting group was then removed with piperidine to afford compounds **6** and **7** in good yields (93 % and 82 % respectively). [28]

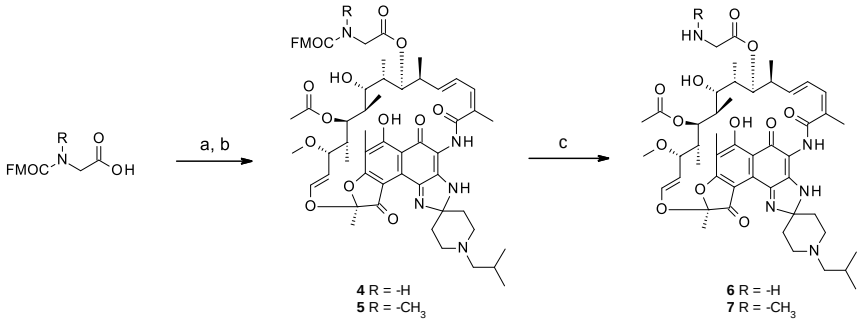

Scheme 2. Synthesis of intermediates **6** and **7**. Reagents and conditions; (a) PivCl, Pyridine, THF, RT; (b) Rifabutin, Pyridine, DMAP, THF, RT, 73-74 %; (c) 20 % Piperidine in THF, RT, 82-93 %.

Intermediates **9a-9h** were prepared in parallel following a two-step procedure: Fmoc-protected amino acids were condensed with glycine *tert*-butyl ester using 1-[(1-(Cyano-2-ethoxy-2-oxoethylideneaminooxy) dimethylaminomorpholino)] uronium hexafluorophosphate (COMU) as coupling agent (Scheme 3) to afford compounds **8a-8h**. The *tert*-butyl group was removed in acidic conditions to obtain the carboxylic acids **9a-h**. The latter were condensed with either **6** or **7** to give intermediates **10a-i**. Finally, the Fmoc protecting-group was cleaved with piperidine in THF to lead to prodrugs **11a-i**.

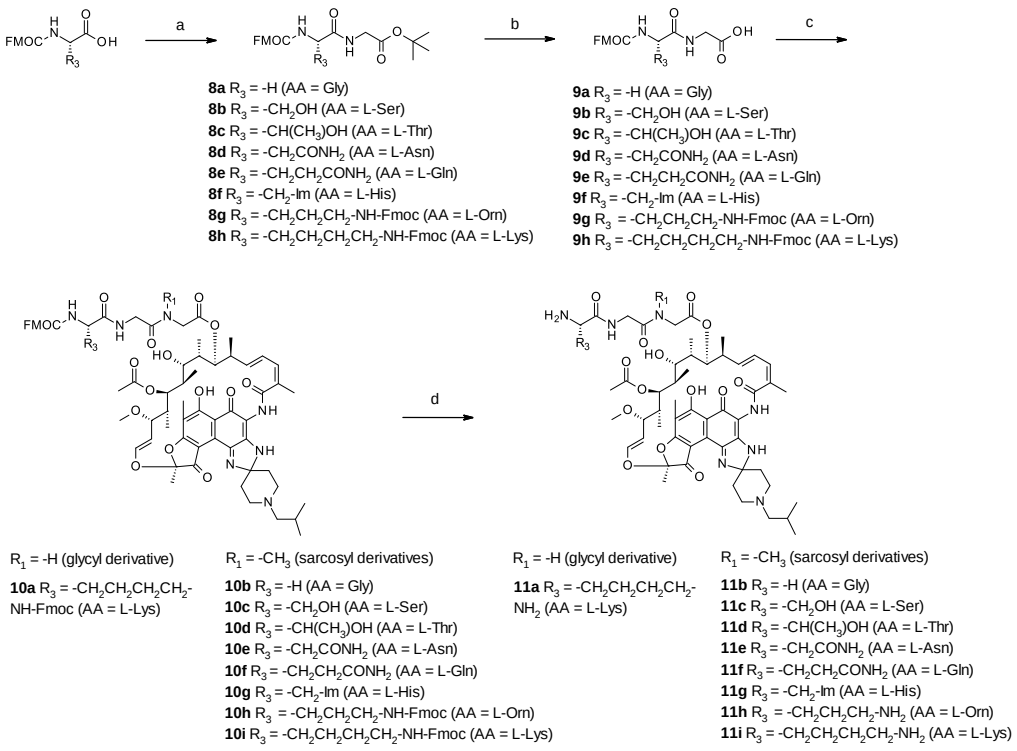

Scheme 3. Synthesis of prodrugs **11a-i**. Reagents and conditions; (a) glycine *tert*-butyl ester, COMU, DIEA, EtOAc or DMF, RT, 53-87 %; (b) TFA in CH_2Cl_2, 36-93 % or HCl in dioxane (**9f**), RT, quant.; (c) **6** or **7,** COMU, DIEA, EtOAc or DMF, RT, 43-79 %; (d) 20 % Piperidine in THF, R.T, 60-100 %.

For the synthesis of **17a** and **17b**, the side chains of Fmoc-Asp and Fmoc-Glu were converted into fluorenylmethyl esters using fluorenylmethanol, dicyclohexylcarbodiimide (DCC) and catalytic amounts of DMAP (Scheme 3).[29] The *tert*-butyl group of **12a-12b** was removed under acidic conditions to give the amino acids **13a-13b**. Then, the same synthetic route as described in Scheme 3 was applied, to obtain the targeted prodrugs **17a** and **17b** in four steps.

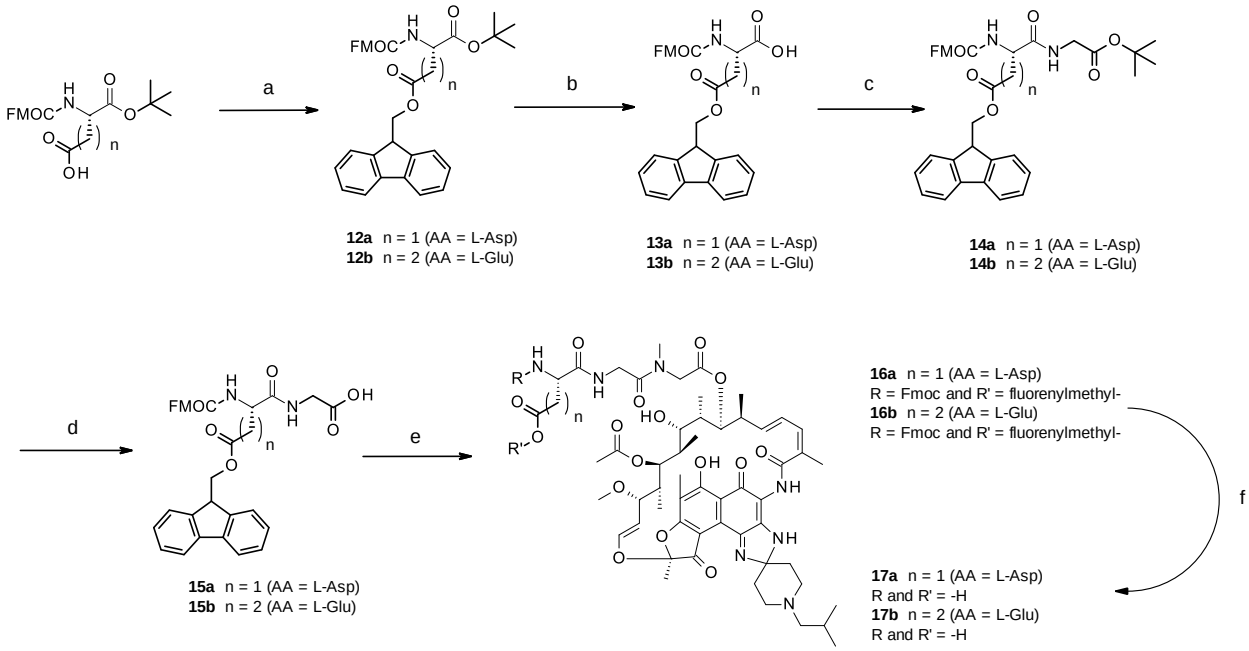

Scheme 4. Synthesis of prodrugs **17a-b**. Reagents and conditions; (a) fluorenylmethanol, DCC, DMAP, CH_2Cl_2, 0 °C to RT, 36-50 %; (b) TFA in CH_2Cl_2, RT, 40-85 %; (c) glycine *tert*-butyl ester; hydrochloride, COMU, DIEA, EtOAc, RT, 81-88 %; (d) TFA in CH_2Cl_2, RT, 74-89 %; (e) **7,** COMU, DIEA, DMF, RT, 57-71 %; (f) 20 % Piperidine in THF, RT, 70-100 %.

Compounds **21a** and **21b** were prepared in three or four steps. **18** was obtained by condensing Fmoc-Lys(Fmoc)-OH and 1*H*-benzotriazole using propylphosphonic anhydride (T3P), then was allowed to react with proline in a mixture of acetonitrile and water (Scheme 5) to give **19a**. **19b** was obtained by adding *N*-ε-Fmoc-lysine in a solution of Fmoc-Lys(Fmoc)-OH in DMF, which had been pre-activated with COMU. Dipeptides **19a-b** were coupled with intermediate **7**, followed by the cleavage of the Fmoc protecting groups to afford prodrugs **21a** and **21b**.

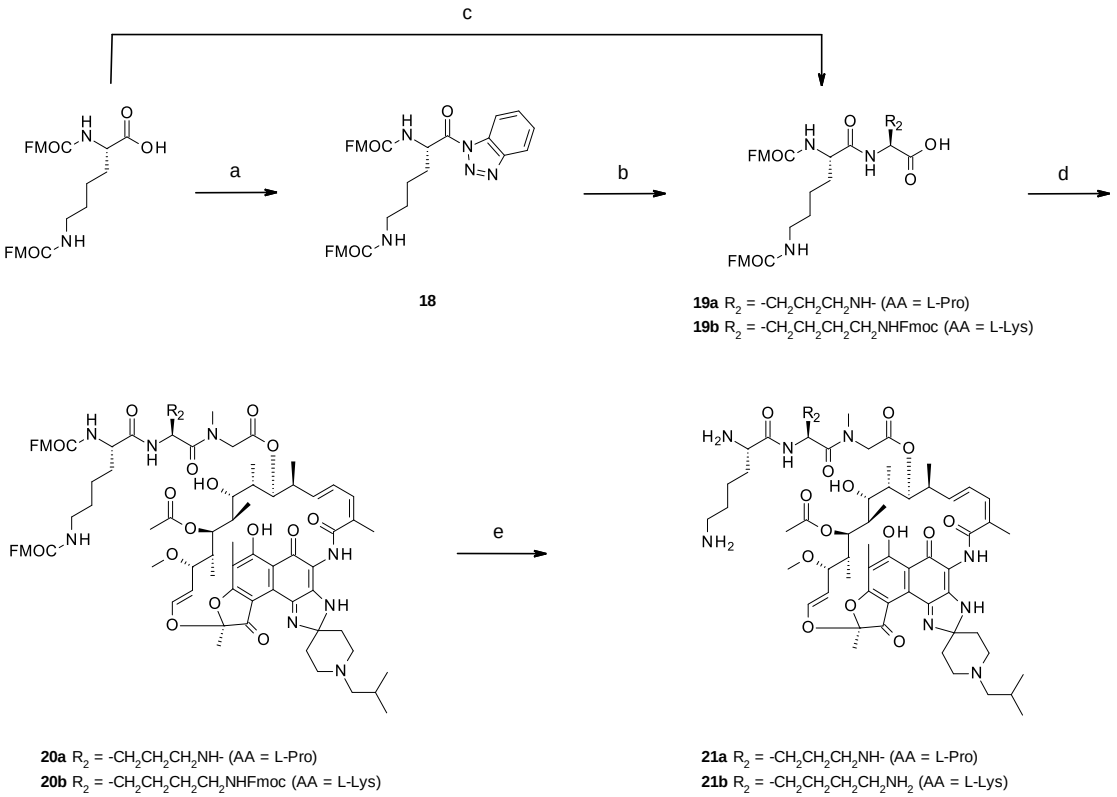

Scheme 5. Synthesis of prodrugs **21a-b**. Reagents and conditions; (a) 1*H*-benzotriazole, T3P, DIEA, EtOAc, RT, 89; (b) L-Pro-OH, Et_3N, H_2O/CH_3CN, RT, 30 %; (c) COMU, L-Lys(Fmoc)-OH, DIEA, DMF, RT, 33 %;(d) **7**, COMU, DIEA, EtOAc or DMF, RT, 17-52 %; (e) 20 % Piperidine in THF, RT, 88-94 %.

2.1.2. Synthesis of type A rifabutin phosphate prodrugs

The synthesis of the prodrug **25** (Scheme 6) was performed in a 4-steps synthesis. Triallylphopshite was first converted into the diallyl phosphoriodidate intermediate using molecular iodine, which is then allowed to react with *tert*-butyl glycolate in presence of DMAP to give **22**. [30] The *tert*-butyl group was then removed under acidic conditions to give **23**. The carboxylic acid **23** was coupled with **7** using COMU to give a mixture of the desired product **24a** and the mono-deprotected compound **24b**. The complete deprotection of **24a** and **24b** was achieved in the presence of $Pd(PPh_3)_4$ as catalyst and morpholine as carbocation scavenger to afford **25**. [31]

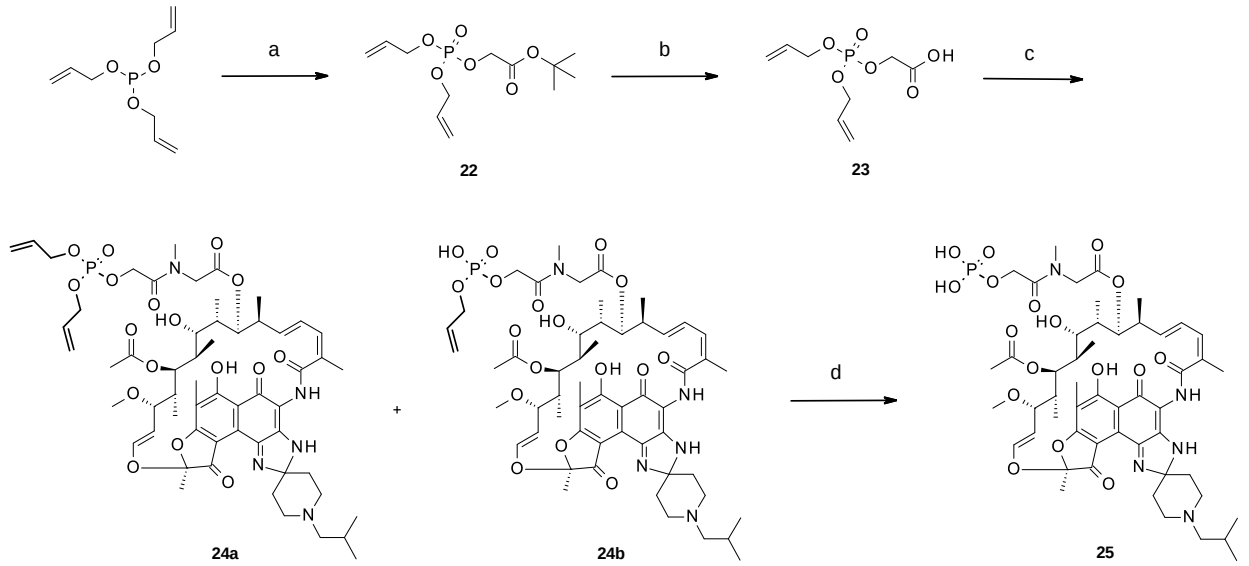

Scheme 6. Synthesis of prodrug **25**. Reagents and conditions; (a) I_2, *tert*-butyl glycolate, DMAP, CH_2Cl_2, 0 °C to RT, 68 %; (b) TFA in CH_2Cl_2, RT, quant.; (c) **7**, COMU, DIEA, EtOAc, RT; (d) $Pd(PPh_3)_4$, morpholine, CH_2Cl_2, RT, 38 %.

2.1.3. Synthesis of type A rifabutin ester prodrugs

The synthesis of prodrug **29** is described in Scheme 7**.** The first step consisted of the acylation of tert-butyl glycolate with chloroacetyl chloride to give the chlorine derivative **26**. The latter was reacted with dimethylamine to give **27**, which was then deprotected with HCl in dioxane to give the carboxylic acid **28**. Finally, coupling with sarcosyl-rifabutin **7** afforded the prodrug **29**.

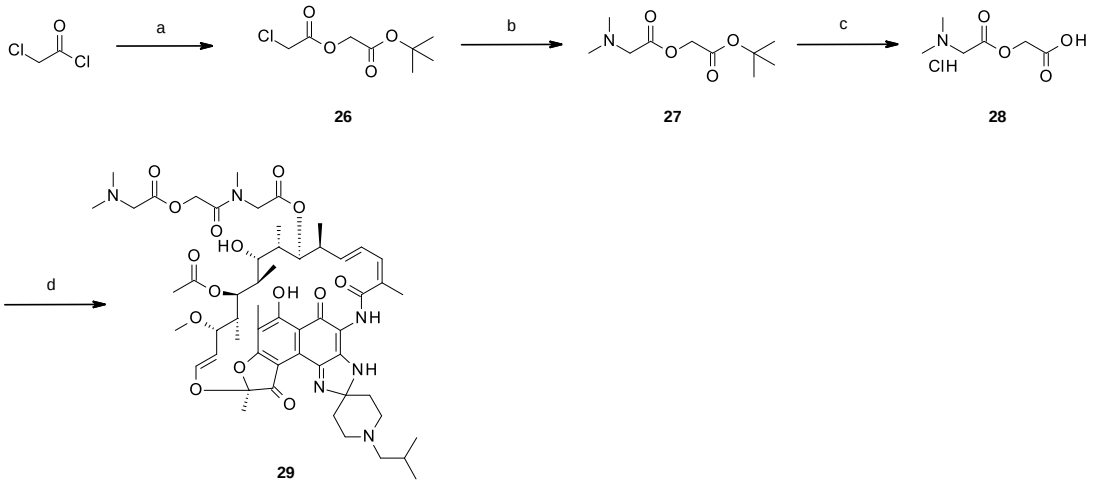

Scheme 7. Synthesis of prodrug **29**. Reagents and conditions; (a) *tert*-Butyl glycolate, pyridine, CH_2Cl_2, 0 °C to RT, 90 %; (b) Dimethylamine, K_2CO_3, CH_3CN, RT, 59 %; (c) 25 % TFA in CH_2Cl_2 then HCl 4N in dioxane, RT, 91 %; (d) **7**, COMU, DIEA, DMF, RT, 65 %.

2.2. Synthesis of type B phosphate prodrugs

The type B phosphate prodrugs were designed to incorporate a self-immolative spacer (*p*-hydroxybenzylalcohol for compound **33** or "trimethyl lock" for compound **43**) between the solubilizing group, here the phosphate, and the labile glycyl-sarcosyl linker (Fig 3).

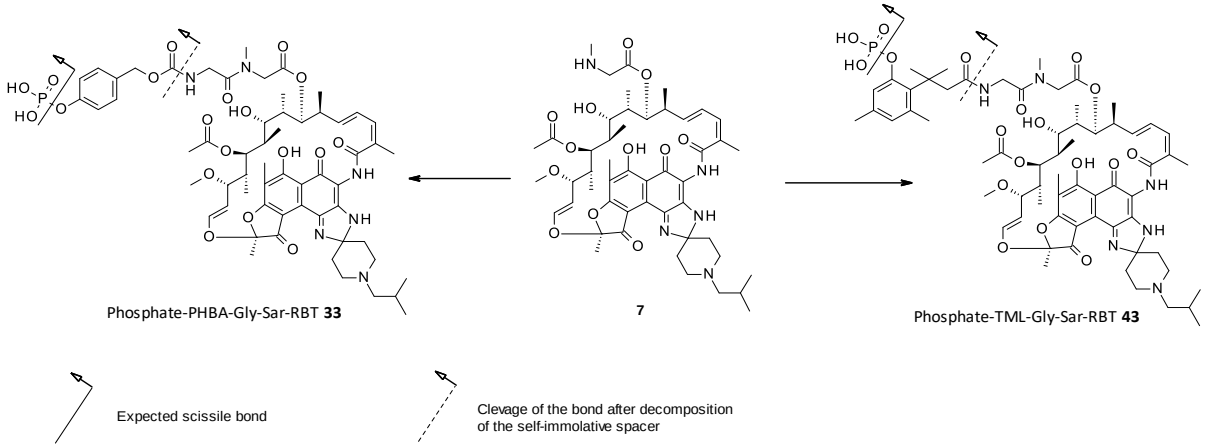

Fig 3. Description of the targeted type B phosphate prodrugs **33**, containing a *p*-hydroxybenzylalcohol spacer, and **43**, containing a "trimethyl lock" spacer.

The prodrug **33** was synthesized starting from **30** (Scheme 8). Compound **30** was obtained from the reaction between diallyl phosphoriodidate, obtained as previously described from triallylphosphite, and 4-hydroxybenzaldehyde, followed by reduction of the aldehyde using

sodium borohydride. [32] The alcohol was allowed to react with 4-nitrophenyl chloroformate to give the corresponding activated carbonate, used to *N*-carbamoylate glycine and to afford compound **31**. Similar to the procedure described above for compound **25**, the coupling with intermediate **7** followed by the deprotection of allyl groups afforded the prodrug **33**.

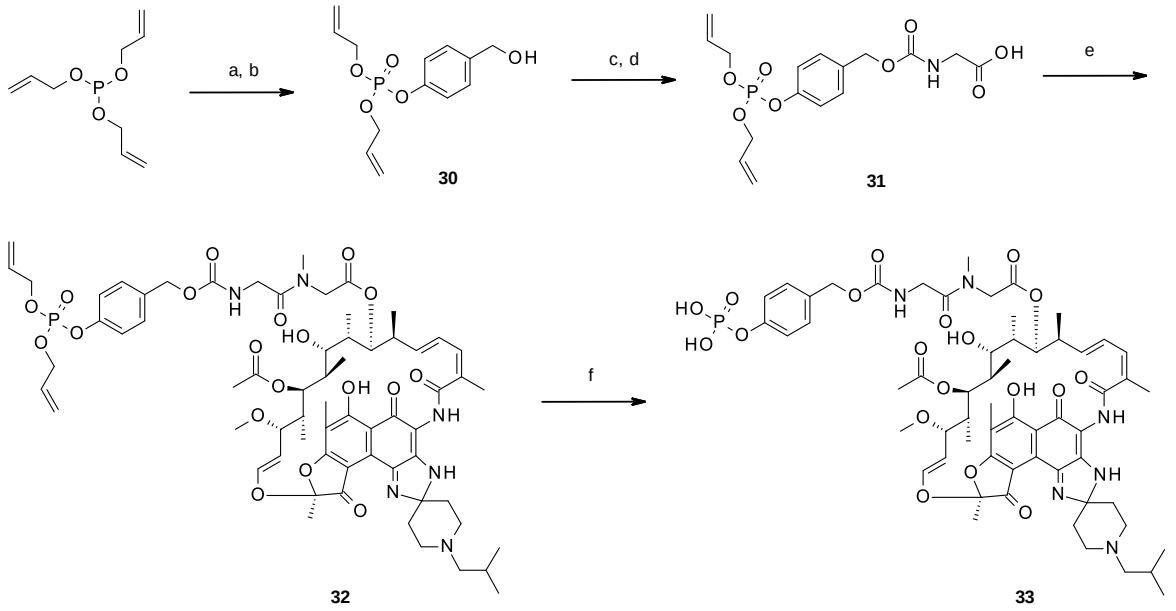

Scheme 8. Synthesis of prodrug **33**. Reagents and conditions; (a) I_2, 4-hydroxybenzaldehyde, DMAP, CH_2Cl_2, 0 °C to RT; (b), $NaBH_4$, THF, 0 °C to RT, 69 % over 2 steps; (c) 4-Nitrophenyl chloroformate, pyridine, CH_2Cl_2, 0 °C to RT; (d) Glycine, Et_3N, CH_3CN/H_2O, RT, 35 % over 2 steps; (e) **7**, COMU, DIEA, EtOAc, RT, 81 %; (f) $Pd(PPh_3)_4$, morpholine, CH_2Cl_2, RT, 86 %.

The synthesis of the prodrug **43** incorporating a “trimethyl lock” linker was performed in 10 steps (Scheme 9). Reaction between 3,5-dimethylphenol and methyl 3,3-dimethylacrylate in methylsulfonic acid under reflux afforded the dihydrocoumarine **34**. [33] Reduction of the lactone with lithium aluminium hydride ($LiAlH_4$) gave the alcohol **35**, [34] which was then protected as silyl ether with *tert*-butyldimethylsilyl chloride (TBDMSCl) to afford **36**. [35] However the latter did not react with diallyl phosphoriodidate in presence of DMAP as previously described. This observation might be explained by the presence of the two methyl substituents on the phenyl ring, making the arene richer in electrons and rendering the phenol more hindered. To circumvent this issue, DMAP was replaced by a stronger base, sodium hydride (NaH), and the deprotected diallyl phosphate **37** was obtained. Classicaly for “trimethyl lock” synthesis, the alcohol is then converted to carboxylic acid with strong oxidants, such as Jones reagent. [35] These harsh conditions were not

suitable due to the presence of the allyl groups. Therefore, aldehyde intermediate **38** was obtained in milder conditions using Dess-Martin periodinane (DMP), [37] which was further oxidized *via* a Pinnick reaction, using sodium chlorite ($NaClO_2$), monosodium phosphate (NaH_2PO4) and resorcinol as a scavenger of hypochlorous acid to afford compound **39**. [38] Finally the same synthetic route as described in Scheme 8 was followed to obtain the prodrug **43**.

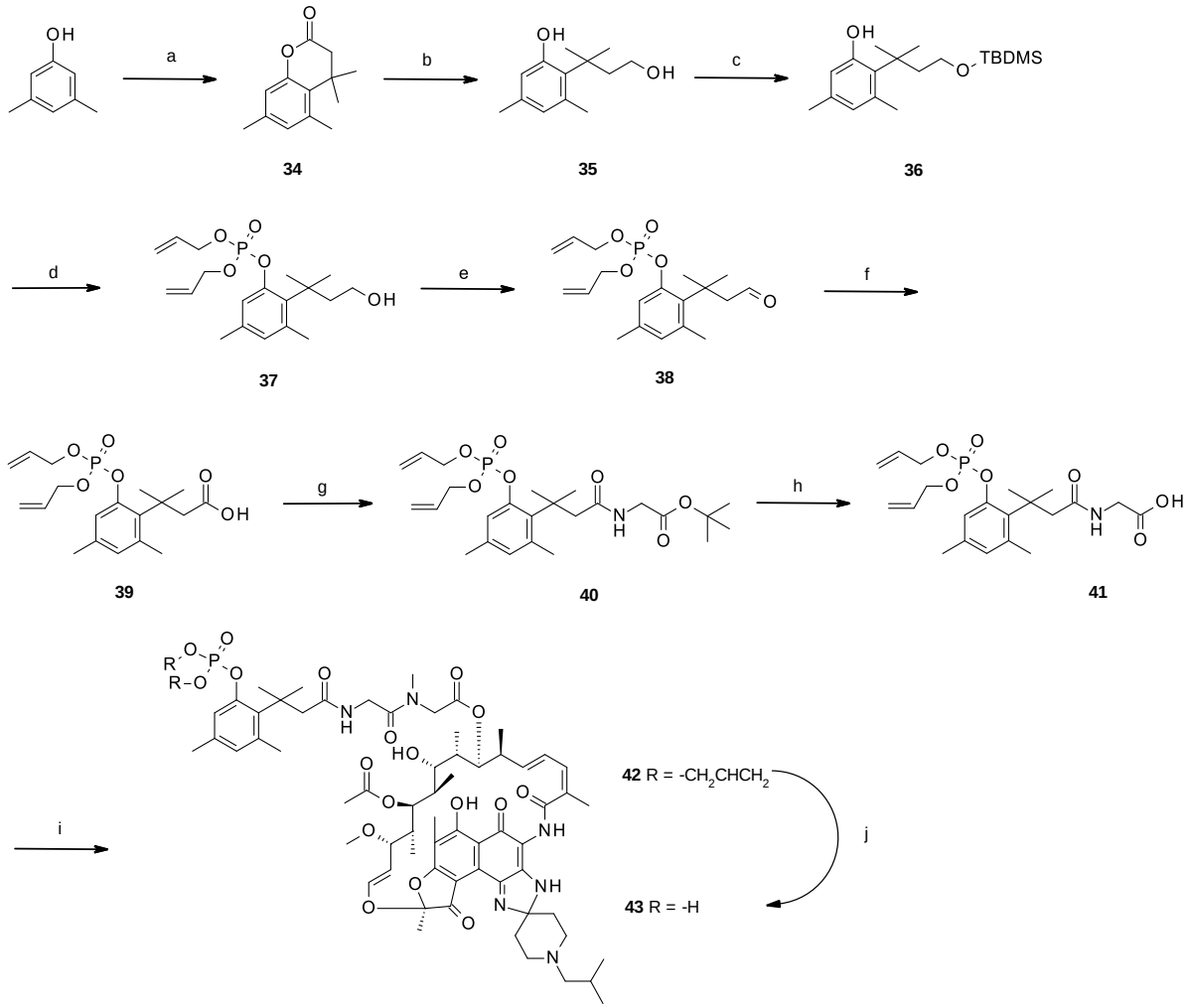

Scheme 9. Synthesis of prodrug **43**. Reagents and conditions; (a) Methyl 3,3-dimethylacrylate, CH_3SO_3H, 70 °C, 78 %; (b) $LiAlH_4$, THF, 0 °C to RT, 45 %; (c) TBDMSCl, imidazole, DMF, 0 °C to RT, 90 %; (d) Triallylphosphite, I_2, NaH 0°C to RT, 57 %; (e) DMP, CH_2Cl_2, 0 °C to RT, 94 %; (f) $NaClO_2$, resorcinol, NaH_2PO_4, H_2O/*t*-BuOH, RT, 81 %; (g) glycine *tert*-butyl ester; hydrochloride, COMU, DIEA, EtOAc, RT, 79 %; (h) TFA, CH_2Cl_2, RT, quant.; (i) **7**, COMU, DIEA, EtOAc, RT, 65 %; (j) $Pd(PPh_3)_4$, morpholine, CH_2Cl_2, RT, 11 %.

3. Results and discussion

3.1. Human plasma stability

To investigate the stability of the prodrugs and their ability to release rifabutin, compounds were first incubated for 6h, at 37°C, in human plasma. The release of rifabutin was monitored by LC-MS. Prodrugs that showed a significant release of rifabutin were then tested, in duplicate, in a kinetic study, where the quantitative dosing of rifabutin was monitored by LC-MS/MS together with the remaining percentage of prodrug and key intermediates.

3.1.1. Type A amide prodrugs

The influence on plasma stability of the nature of amino acids incorporated in the prodrug structures was studied to establish structure-reactivity relationships (Table 2). In the AA_3-Gly-Gly-RBT series, Lys-Gly-Gly-RBT **11a** showed only low release of rifabutin (6%), despite a very low amount of remaining prodrug (6%). LC-MS analysis confirmed the cleavage of the amide bond between the two glycines, leading to the release of the stable glycyl-rifabutin intermediate **6** (Fig. S2). The introduction of a non-proteogenic amino acid, sarcosine, allowed circumventing this issue. In contrast, Lys-Gly-Sar-RBT **11i** showed the highest percentage of rifabutin release after 6h of incubation (95%) together with a percentage of remaining prodrug of 0.6 % ± 0.06 (Fig. S3). The formation of sarcosyl-rifabutin intermediate **7** was not observed. A lower level of released rifabutin (45%) was measured with Orn-Gly-Sar-RBT **11h**. However, because of its chemical instability observed after deprotection, **11h** was not considered for further investigations. In this series, the introduction of amino acids with a neutral side chain at physiological pH such as glycine (Gly-Gly-Sar-RBT, **11b**), serine (Ser-Gly-Sar-RBT, **11c**), threonine (Thr-Gly-Sar-RBT **11d**), asparagine (Asn-Gly-Sar-RBT, **11e**), and glutamine (Gln-Gly-Sar-RBT, **11f**), or with a partially protonated or totally deprotonated side-chains (His-Gly-Sar-RBT, **11g**; Asp-Gly-Sar-RBT, **17a**; Glu-Gly-Sar-RBT, **17b**) led to stable prodrugs (< 24% of rifabutin release at 6h).

Based on these initial results, a new series of tripeptidic prodrugs were designed where lysine and sarcosine were used as terminal and first amino acids respectively. Only the second amino acid was modified. Two prodrugs were synthesized with the general structure Lys-AA_2-Sar-RBT, where AA_2 is a proline (**21a**) or a lysine (**21b**). Both prodrugs appeared more stable than **11i**.

The role of the sarcosine appeared to be crucial to avoid cleavage between AA_1 and AA_2. As expected, not all terminated amino acids (AA_3) are equally cleaved. Among compounds from **11b** to **17b**, only lysine in **11i** is efficiently cleaved, allowing the rapid release of rifabutin.

Table 2. General structure of type A amide prodrugs **11a-21b** and percentage of rifabutin release at 6h in human plasma.

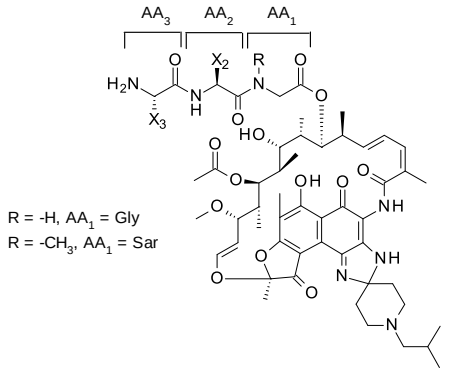

Compound	Strucuture AA_3-AA_2-AA_1-RBT	Qualitative monitoring of rifabutin[a]	Dosing of rifabutin and monitoring of the remaining prodrug[b]		
		% of rifabutin release at 6 h	% of rifabutin release at 6 h	Time to achieve 50% of rifabutin release (min)	% remaining of prodrug at 6 h
11a	Lys-Gly-Gly-RBT	6	6	N.D.[c]	3 ± 0.02
11b	Gly-Gly-Sar-RBT	20	-[d]	-	-
11c	Ser-Gly-Sar-RBT	24	-	-	-
11d	Thr-Gly-Sar-RBT	17	-	-	-
11e	Asn-Gly-Sar-RBT	13	-	-	-
11f	Gln-Gly-Sar-RBT	13	-	-	-
11g	His-Gly-Sar-RBT	18	-	-	-
11h	Orn-Gly-Sar-RBT	45	-	-	-
11i	Lys-Gly-Sar-RBT	79	95 ± 2.1	80 ± 0.1	0.6 ± 0.06
17a	Asp-Gly-Sar-RBT	11	-	-	-
17b	Glu-Gly-Sar-RBT	7	-	-	-
21a	Lys-Pro-Sar-RBT	0	-	-	-
21b	Lys-Lys-Sar-RBT	25	-	-	-

[a] Experiments were performed in simplicate and the release of rifabutin was monitored by LC-MS.

[b] Experiments were performed in duplicate and the release of rifabutin and the remaining prodrug were dosed by LC-MS/MS. The reaction proceeds according to first order kinetics.

[c] N.D.: not determined, since rifabutin release was only 6 %.

[d] "-": Dosing of rifabutin and monitoring of the remaining prodrug were not performed since only a low release of rifabutin was observed during the qualitative monitoring of rifabutin assay.

3.1.2. Type A phosphate and ester prodrugs

Together with amide prodrugs, the stability of type A phosphate and ester prodrugs was also measured in human plasma (Table 3). A high release of rifabutin (95% and 78%) from the phosphate prodrug **25** and the ester prodrug **29** was measured after 6h of incubation (Fig. S4 and S5). This was further confirmed in a kinetic study, where the time to achieve 50% of rifabutin release was respectively 290 and 281 min. However, after 6h, the conversion of **25** and **29** to rifabutin was not complete which is attributed to the slower intramolecular cylization of the released alcohol intermediate upon phosphate and ester cleavage, compared to the amino intermediate (Fig. S7).

3.1.3. Type B Phosphate prodrugs

Self-immolative linkers (*p*-aminobenzylalcohol, PABA and "trimethyl lock", TML) were also introduced to bridge Gly-Sar-RBT with the phosphate group. Interestingly, an almost total liberation of rifabutin was obtained at 6h (86 %) with **33** (Fig. S6). Prodrug **43** proved to be stable, in contrast to some examples found in the literature. [39]

Table 3. Percentage of rifabutin release at 6h in a human plasma with type A and B phosphate prodrugs (**25**, **33**, **43**) and type A ester prodrug (**29**).

	Qualitative monitoring of rifabutin[a]	Dosing of rifabutin and monitoring of the remaining prodrug[b]		
Compound	% of release at 6h	% of rifabutin release at 6h	Time to achieve 50% of rifabutin release (min)	% remaining of prodrug at 6 h
25	95	59 ± 0.3	290 ± 5.5	30 ± 1.6
29	78	67[c]	281[c]	36[c]
33	90	86 ± 0.4	188 ± 5.6	9 ± 1.4
43	9	-[d]	-	-

[a] Experiments were performed in simplicate and the release of rifabutin was monitored by LC-MS.

[b] Experiments were performed in duplicate and the release of rifabutin and the remaining prodrug were dosed by LC-MS/MS.

[c] Only one of the two samples was analyzed.

[d] "-": Dosing of rifabutin and monitoring of the remaining prodrug were not performed since only a low release of rifabutin was observed during the qualitative monitoring of rifabutin assay.

3.2. Water solubility

Based on plasma stability results (Tables 2 and 3), the most promising prodrugs from each category were selected: type A prodrugs **11i** and **29**, and type B prodrug **33**. The solubility of these prodrugs was assessed in PBS (pH 7.4). For basic prodrugs **11i** and **29**, the solubility was also measured in aqueous HCl (26 mM).

Thanks to the presence of a primary amine, the prodrug **11i** was highly soluble in PBS (>50 mg/mL) compared to rifabutin (0.2-0.9 mg/mL). The compound was also twice as soluble as rifabutin in aqueous HCl (26 mM) (respectively 34.4 mg/ml and 17.7 mg/mL). Regarding **29**, the compound was as soluble as rifabutin, either in PBS (0.6 mg/mL) or in aqueous HCl (26 mM) (12.2 mg/mL). The presence of an additional dimethylamino group in the structure of prodrug **29** was not sufficient to improve its water solubility. The introduction of a phosphate group conferred also to **33** an improved water solubility in PBS (4.5 mg/mL) compared to rifabutin.

Table 4. Solubility of prodrugs **11i**, **29** and **33** in PBS (pH 7.4) and HCl (26 mM).

Compound	Solubility in PBS (pH 7.4) (mg/mL)	Solubility in HCl (26 mM) (mg/mL)
Rifabutin	0.2-0.9	17.7
11i	> 50	34.4
29	0.7	12.2
33	4.5	-[a]

[a] Water solubility of phosphate prodrug **33** was not measured in acidic solution.

3.3. *A. baumanni* and *S. aureus* growth inhibition

Serum supplementation is required for hyperactivity of rifabutin against *A. baumannii* but also for the cleavage of the prodrugs and release of rifabutin. Conversely, MIC of rifabutin against *S. aureus* is not affected by the absence of serum supplementation in CAMHB.

Therefore, the antibacterial activity of prodrugs **11i**, **29** and **33** were determined against *S. aureus* in the growth medium CAMHB prior incubation with serum in order to verify that the uncleaved prodrugs were not active by themselves, and after incubation to compare MICs with rifabutin (Table 5). The prodrugs showed 64- to 2048-fold reduced potency compared to rifabutin when

tested without serum preincubation while they showed a 80- to 512-fold increased potency after preincubation in serum, leading to similar activity as rifabutin.

Likewise, prodrugs **11i**, **29** and **33** tested against *A. baumannii* in CAMHB supplemented with human serum (HS) were able to quantitatively release rifabutin as the three solutions had similar apparent MIC and inhibited the growth of *A. baumannii* in the same order of magnitude as rifabutin (Table 5).

Altogether, these results confirm the strong serum/plasma-mediated release of rifabutin with these prodrugs.

Table 5. MIC of prodrugs **11i**, **29** and **33** against *A. baumannii* in CAMHB supplemented with human serum (HS) and against *S. aureus* in CAMHB before or after 6 hours incubation in HS. Experiment was performed in triplicate.

Compound	MIC on *A. baumannii* in CAMHB + 50% HS (µg/mL)	MIC on *S. aureus* in CAMHB (µg/mL)	
		without HS preincubation	with 6h HS preincubation
Rifabutin	0.00025	0.016	0.03
11i	0.001	16	0.06
29	0.001	1	0.06
33	0.001	32	0.06

3.4. Mouse plasma stability

Before starting *in vivo* PK studies in mice, the stability of the prodrugs **11i**, **29** and **33** in mouse plasma was measured to assess any interspecies variability. [40,41]

Rifabutin release of respectively 74 %, 85 % and 100 % were determined for prodrugs **11i**, **29** and **33** after 6 hours respectively (Fig. 4). Values were higher compared to those obtained in human plasma stability assay for **29** and **33** (respectively 67 % and 86 %), which is line with the presence of higher level of enzymes in mouse plasma. [42] Interestingly, the amide prodrug **11i** was more stable in mouse plasma than in human plasma (95 % of rifabutin release in the latter).

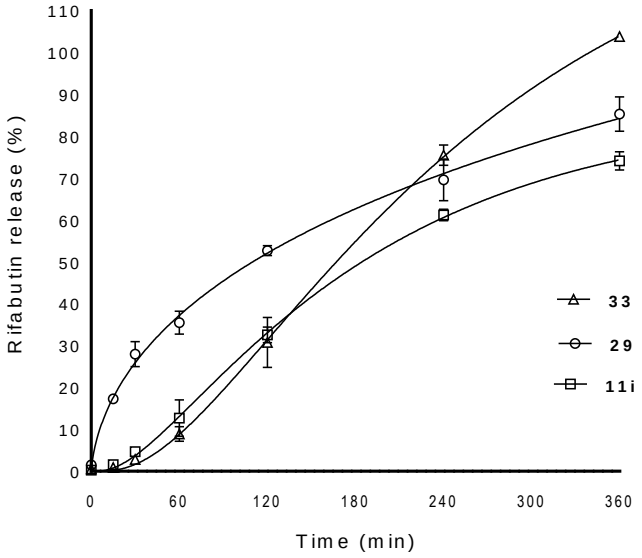

Fig 4. Rifabutin release in mouse plasma from prodrugs **11i**, **29** and **33**. Experiment was performed in duplicate.

The rifabutin release from the prodrugs is the result of two first order kinetics reactions. First, the cleavage of the scissile bond generates the key nucleophilic intermediate and subsequently the intramolecular cyclization from this intermediate triggers the release of rifabutin.

The sigmoidal release of RBT observed for prodrugs **11i** and **33** suggests that the rate of the two steps is equivalent. By fitting the data to a sum of exponentials, the rate constants k_1 of the cleavage reaction and k_2 of the intramolecular cyclization have been determined. [43] As expected, the two steps proceed with similar rates for both prodrugs (k_1 = 0.007 min^{-1} and k_2 = 0.011 min^{-1} for **11i**; $k_1 = k_2$ = 0.011 min^{-1} for **33**). Conversely, the exponential release of rifabutin observed with compound **29** suggests that the cyclization proceeds much slower than the enzymatic cleavage. This is in line with the plasma stability experiments we performed where the amine intermediate was not detectable after 6 h as opposed to the alcohol intermediate, indicating that the cyclization rate was slower for the latter (Fig. S7).

3.5. Pharmacokinetic studies

The three prodrugs **11i**, **29** and **33** were assessed in a pharmacokinetic study in female CD1 mice alongside rifabutin. For each compound, the plasma concentration of rifabutin was monitored by LC-MS/MS over 24 h, after IV bolus injection (Fig. 5A). The doses used for the three prodrugs **11i, 29** and **33,** respectively 6.5 mg/kg, 6.5 mg/kg and 7.0 mg/kg, were chosen to be equimolar to a

dose of 5 mg/kg of rifabutin (assuming 100% release), a dose at which rifabutin was shown to be active in an immunocompetent *A. baumannii* pneumonia infection mice model in contrast to rifampicin. [7,44]. The basic compounds (**11i**, **29** and rifabutin) were formulated in 0.9 % NaCl with 26 mM HCl to optimize aqueous solubility, particularly for rifabutin, for wich 10 % DMSO was added to also facilitate dissolution. The phosphate prodrug **33** was formulated in PBS (pH 7.4).
The chemical stability of the prodrugs was evaluated in the formulation media at room temperature over 6h. The three compounds were confirmed to be stable, with a remaining percentage of respectively 99 % ± 0.8 %, 101 % ± 0.7 % and 101 % ± 0.6 % (Table S1).

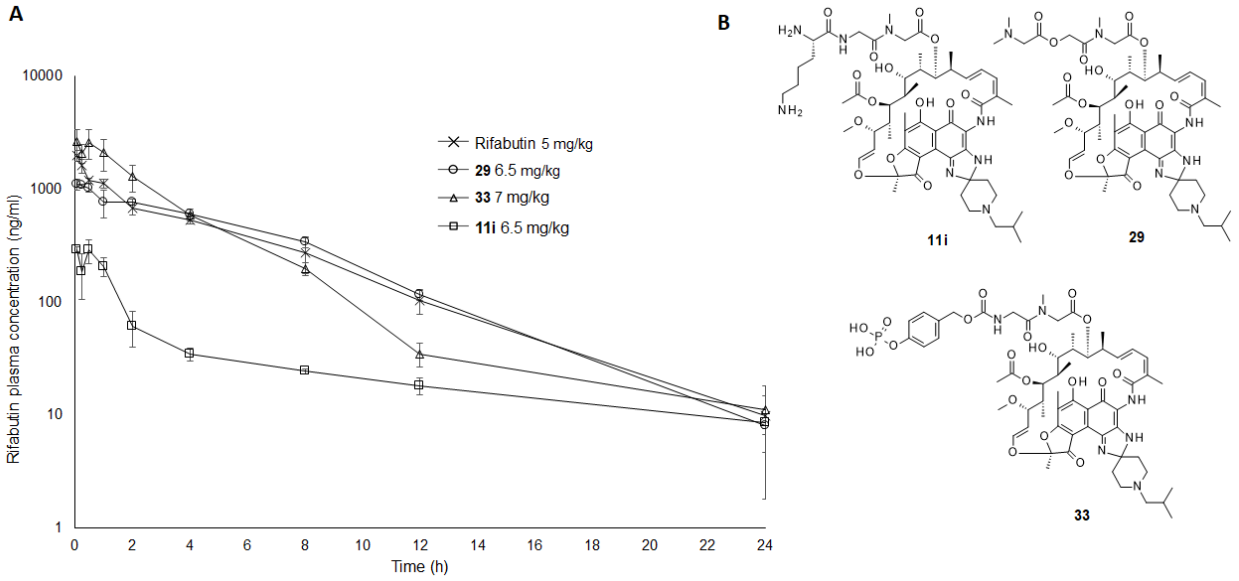

Fig. 5. A) Rifabutin plasma concentration over time after IV injection of rifabutin and prodrugs **11i**, **29** and **33** in female CD1 mice. Experiment was performed in duplicate **B)** Structures of prodrugs **11i**, **29** and **33**.

For the three prodrugs, the maximum blood concentration of released rifabutin was reached after 5 min (Table 6). The phosphate prodrug **33** showed a C_{max}= 2.7 µg/mL slightly higher than the initial concentration of rifabutin (C_0 = 2.2 µg/mL). The release of rifabutin from prodrug **29** was lower by a factor 2 with a C_{max}= 1.1 µg/mL. Finally, the prodrug **11i** showed a low release of rifabutin with a Cmax = 0.3 µg/mL. The same tendency was observed for exposure with IV administration of the prodrugs **33** and **29** leading to $AUC_{0-\infty}$ of 8.2 µg.h/mL and 6.7 µg.h/mL, which is equivalent to that of rifabutin ($AUC_{0-\infty}$ = 6.6 µg.h/mL), while exposure of rifabutin from **11i** was lower (1.0 µg.h/mL).

The two prodrugs **29** and **33** have a pharmacokinetic profile almost identical to rifabutin, indicating a fast release of rifabutin *in vivo*. This was not the case with **11i**, which seems more stable *in vivo* than *in vitro* (**Fig. 4**) and/or could have a clearance faster than the liberation of rifabutin.

Table 6. Pharmacokinetic parameters for prodrugs **11i**, **29** and **33** in female CD1 mice.

PK parameters	**Rifabutin** (5 mg/kg)	**11i** (6.5 mg/kg)	**29** (6.5 mg/kg)	**33** (7.0 mg/kg)
C_0[a] or C_{max}[b] (µg/mL)	2.2	0.3	1.1	2.7
t_{max}[c] (h)	-[f]	0.083	0.083	0.083
$t_{1/2z}$[d] (h)	3.4	10.7	3.0	2.9
$AUC_{0-\infty}$[e] (µg.h/mL)	6.6	1.0	6.7	8.2

[a] C_0: initial calculated concentration of rifabutin

[b] C_{max}: maximum blood concentration of rifabutin

[c] t_{max}: time when the blood concentration of rifabutin is maximum

[d] $t_{1/2z}$: terminal elimination half-life

[e] $AUC_{0-\infty}$: area under the concentration-time curve extrapolated to infinity

[f] t_{max} of rifabutin corresponds to t_0

3. Conclusion

Rifabutin has recently been shown to have potent *in vitro* and *in vivo* activity against *A. baumannii* [7,43,44]. Given its limited oral bioavailability and low solubility, the development of water-soluble prodrugs of rifabutin would allow its intravenous administration at higher doses, which could result in increased AUC compared to oral administration at the same dose. This increased exposure would positively influence the AUC/MIC-dependent killing power of rifabutin, leading to increased efficacy. We therefore worked on the synthesis, physicochemical evaluation and *in vitro* stability study of rifabutin prodrugs, differing in the nature of the chemical bond (amide, phosphoester or ester) cleaved by plasma enzymes and incorporating or not self-immolating linkers.

In total, 17 prodrugs were synthesized. Evaluation of their stability in human plasma showed that the tripeptide prodrug **11i**, the ester prodrug **29** and the phosphate prodrug **33** were the most effective in releasing rifabutin rapidly. Compound **11i** showed the highest release of rifabutin over 6 h in human plasma, with half the drug released after 80 min. The prodrugs were also tested against *A. baumannii* in the presence of human serum. All three prodrugs showed potent activity comparable to that of rifabutin, indicating quantitative drug release under microbiological

conditions. With regard to water solubility, the presence of a lysine in the structure of **11i** improved solubility in PBS and in aqueous HCl solutions. The phosphate prodrug **33** was also more soluble than rifabutin in PBS. However, despite the introduction of a basic dimethylglycine, fully protonated at physiological pH, the solubility of prodrug **29** remained in the same range as rifabutin. We also showed that all three compounds were stable in the formulation medium used for the pharmacokinetic studies. Analyses of mouse plasma samples after intravenous injection indicated a rapid and complete conversion of prodrugs **29** and **33** to rifabutin in blood, which was consistent with the *in vitro* conversion in mouse plasma. We also found that the pharmacokinetic parameters (AUC and Cmax) of rifabutin released from prodrugs **29** and **33** were similar to those of the drug based on an equimolar dosage. For prodrug **11i**, the total exposure of rifabutin released was lower, confirming the higher stability observed *in vitro* in mouse plasma with this prodrug.

Based on water solubility and *in vitro* stability in human plasma, **11i** appears to be the most promising prodrug. In pharmacokinetic studies in mice, compound **33** showed the best prodrug profile for the development of an intravenous formulation of rifabutin. Prodrugs of rifabutin are a promising approach to improve the solubility of rifabutin and increase the therapeutic options of this drug. The identification of the enzyme(s) responsible for the cleavage of these prodrugs is under investigation.

4. Materials and Methods

Experiments with replicates were not independent except the procedure for MIC determination.

4.1. Chemistry

Reagents and solvents for synthesis, analysis or purification were purchased from commercial suppliers and used without further purification. Progress of all reactions was routinely monitored by thin layer chromatography (TLC) and/or by High Performance Liquid Chromatography - Mass Spectrometry (HPLC-MS). TLC was performed using Merck® commercial aluminum sheets coated with silica gel 60 F254. Visualization was achieved by fluorescence quenching under UV light at 254 nm or stained by potassium permanganate. Purifications were performed by flash chromatography, reverse chromatography or preparative HPLC. Flash chromatography purifications were done on prepacked columns Reveleris® flash cartridges (40 µm, Büchi® FlashPure or 15-40 µM, Macherey-Nagel® Chromabond) under pressure with an Interchim Puriflash® 430 instrument. Products were detected by UV absorption at 254 nm and by ELSD. Reverse chromatography were done using Combiflash® C18 Rf200 on 4g, 12 g, 24 g or 40 g C18 column. Products were detected by UV absorption at 215 nm and 254 nm. Preparative HPLC were

performed using Varian® ProStar system with an Omnisphere 10 µm C18 column (250 mm x 41.4 mm) Dynamax from Varian, Inc. Mobile phase was a mixture of H_2O (0.1 % of formic acid) and CH_3CN (0.1% of formic acid) and the flow rate was 80 mL/min. Products were detected by UV absorption at 215 nm and/or 254 nm. HPLC-MS analysis was performed on LC-MS Waters Alliance Micromass ZQ 2000 system equipped with a Waters 2747 sample manager, a Waters 2695 separations module, a Waters 2996 photodiode array detector (210-400 nm at a 1.2 nm resolution) and a Waters Micromass ZQ2000 detector (scan 100-800). XBridge C18 column (3.5 µm particle size, dimensions 50 mm x 4.6 mm) was used for HPLC analysis. The injection volume was 20 µL. For a 5 min analysis, the elution was done at pH 3.8 from 100% H_2O/0.1% ammonium formate to 2% H_2O/98% CH_3CN/0.1% ammonium formate over 3.5 min. A flow rate at 2 mL/min was used. For a 30 min analysis, the elution was done at pH 3.8 from 100% H_2O/0.1% ammonium formate to 2% H_2O/98% CH_3CN/0.1% ammonium formate over 7 min. A flow rate at 1 mL/min was used. Purity (%) was determined by reversed phase HPLC, using UV detection (215 and 254 nm).. HRMS analysis were performed on a LCT Premier XE Micromass, using a C18 X-Bridge 3.5 µm particle size column, dimensions 50 mm * 4.6 mm. A gradient starting from 98% H_2O 5 mM ammonium formate pH=3.8 and reaching 100% CH_3CN 5 mM ammonium formate pH=3.8 within 3 min at a flow rate of 1 mL/min was used. NMR spectra were recorded on a Bruker® Avance-300 spectrometer or Bruker® Avance-500 spectrometer. The results were calibrated to signals from the solvent as an internal reference [e.g. 7.26 (residual $CDCl_3$) and 77.16 ($CDCl_3$) ppm, 2.50 (residual DMSO-d_6) and 39.52 (DMSO-d_6) ppm for ^1H and ^{13}C NMR spectra, respectively]. Chemical shifts (δ) are in parts per million (ppm) downfield from tetramethylsilane (TMS). The assignments were made using one-dimensional (1D) 1H and 13C spectra and two-dimensional (2D) HSQC-DEPT, COSY and HMBC spectra. NMR coupling constants (*J*) are reported in Hertz (Hz), and splitting patterns are indicated as follows: s (singlet), brs (broad singlet), d (doublet), dd (doublet of doublet), ddd (double of doublet of doublet), dt (doublet of triplet), t (triplet), td (triplet of doublet), q (quartet), m (multiplet).

4.2. Procedure for stability in human plasma studies

4.2.1. Experience in singlicate: monitoring of rifabutin release

Human plasma was obtained from BioIVT (mix gender, lithium heparin, BRH1407403). A solution of 10 mM of the tested compounds and rifabutin was prepared in MeOH, then was diluted 100 times with 400 µL of plasma which had been pre-incubated for 10 minutes at 37 °C. The samples were shaken with a ThermoMixer at 37 °C. The plasma was sampled at t = 0 and t = 6 h, then was diluted 10 times with cold acetonitrile to precipitate the plasma proteins. After centrifugation

at 12 000 rpm at 4 °C for 10 min, the supernatant was recovered and was analyzed by HPLC-MS (full-scan analysis). The AUC of the signal of rifabutin, at m/z $[M+H]^+$ = 847, was determined for the rifabutin sample as well as the tested prodrugs. The percentage release of rifabutin was calculated by doing the ratio between the AUC signal of the rifabutin released by the prodrugs, and the AUC signal of the rifabutin sample.

4.2.2. Experience in duplicate: dosing of rifabutin release and monitoring of prodrugs cleavage

Experiment was performed in duplicate but were not independent. Human plasma was obtained from BioIVT (mix gender, lithium heparin, HMN490326). A solution of 10 mM of the tested compounds and the reference (eucatropine) [45] was prepared in DMSO, then was diluted 1000 times with plasma which had been pre-incubated for 10 minutes at 37 °C. Each sample was prepared in duplicate. The samples were shaken with a ThermoMixer at 37 °C. at selected time (0, 0.25, 0.5, 1, 2, 4 and 6 h), then was diluted 10 times with cold acetonitrile to precipitate the plasma proteins. After centrifugation at 12 000 rpm at 4 °C for 10 min, the supernatant was recovered and was analyzed by UPLC-MS/MS (MRM, parameters bellow). Release of rifabutin was dosed, by quantifying the molecule form a calibration curve. The tested prodrugs and the intermediates were monitored. The experience was validated using eucatropine as reference.
UPLC-MS/MS informations: analysis were performed on Acquity I Class-Xevo TQD with a Waters Acquity BEH C18 column (1.7 µm particle size, dimensions 50 mm x 2.1 mm) (40 °C). The injection volume was 1 µL. For a 5 min analysis, the elution was done at pH 3.8 from 100% H_2O/0.1% ammonium formate to 2% H_2O/98% CH_3CN/0.1% ammonium formate over 2 min. A flow rate at 600 µL/min was used. No internal standard was used. Concerning mass spectroscopy, following parameters were applied: source temperature of 150 °C, desolvatation temperature of 600 °C, acone gas flow of 50 L/h, desolvatation gaz flow of 1200 L/h, capillary voltage of 0,5 kV. For detection of the compounds by ES+ mode, following mass transitions were used: 847.473 > 815.444 (rifabutin), 552.532 > 84.177 (**11i**), 531.468 > 57.956 (**29**), 1205.346 > 1173.516 (**33**).

4.3. Procedure for water solubility measurement

The experiment was performed in singlicate. Solution of the tested compounds were prepared at 10 mg/mL or 50 mg/mL in extradry DMSO. Theoretical solutions of the test compounds were prepared in PBS pH=7.4 or HCl 0.026M at 10 mg/mL (**29** and rifabutin in PBS pH=7.4) or 50 mg/mL (**11i**, **29** and rifabutin in HCl 0.026M, **33** in PBS pH=7.4). Samples were vigorously vortexed

then were shaken at 35 rpm with an intelli-mixer over 24 h at RT. After centrifugation at 12 000 rpm at RT for 10 min, the supernatant was recovered and was filtered. 20 µL were collected then were diluted 2000 times with CH_3CN. The samples were analyzed by UPLC-MS/MS (MRM detection, same parameters than for part 4.2.2 except injection volume: 0.2 µL for prodrugs and 2 µL of rifabutin quantification). Solubility was calculated as follows:

$S = AUC_A/AUC_B \times C$

Where S = water-solubility (mg/mL), AUC_A = AUC of the signal of the tested compound in HCl 0.026M or PBS 7.4, AUC_B = AUC of the signal of the tested compound in DMSO, C = theoretical maximum concentration (mg/mL).

4.4. Procedure for MIC determination

Experience was performed as three independent replicates. The extensively drug resistant HUMC1 strain was used to determine MIC against *A. baumannii*, while the USA300 UAMS-1625 strain was used for MIC against *S. aureus*. MICs were determined using broth the microdilution method following the CLSI guidelines. Briefly, from an overnight culture plate, cells were resuspended in 0.9% (w/v) saline solution and bacterial inoculum was prepared in the respective testing medium with $5x10^5$ CFU/mL. The appropriate volumes of a 10 mg/mL compound solution were directly dispensed in the 96-well assay plate using a digital dispenser to create 2-fold dilution series from 32 µg/mL final concentration. 100 µL of bacterial suspension was finally added to the compounds. Plates were covered and incubated without shaking at 35 °C for 20 hours. MIC was determined visually as the lowest concentration of a compound that prevents visible growth of the bacteria.

As specified in the text, MIC against *A. baumannii* were performed in the Roswell Park Memorial Institute (RPMI) (Sigma, #R8758) medium supplemented with 10% (v/v) of fetal calf serum (FCS) (Gibco, #10500-064) or in cation-adjusted Muller Hinton broth (CAMHB) (BD, #212322) supplemented with 50% (v/v) human serum (HS) (SeraCare, #1830-0002). For MIC against *S. aureus* after HS preincubation, a 10-fold concentrated drug solution of the top concentration tested (32 µg/ml) was preincubated in 100% HS for 6 hours. This solution was then used to manually do the 2-fold dilution series at 10 µl final in the 96-well assay plate and 90 µl of bacteria suspension were added to the compounds. The plate incubation and MIC reading were performed as described above.

4.5. Procedure for stability studies in mouse plasma: monitoring of rifabutin release

Experiment was performed in duplicate but were not independent. Female mouse plasma was obtained from BioIVT (lithium heparin, MSE416139). A solution of 10 mM of the tested compounds and rifabutin was prepared in MeOH, then was diluted 100 times with 400 µL of plasma which had been pre-incubated for 10 minutes at 37 °C. The samples were shaken with a ThermoMixer at 37 °C. The plasma was sampled at selected time (0, 0.25, 0.5, 1, 2, 4 and 6 h), then was diluted 10 times with cold acetonitrile to precipitate the plasma proteins. After centrifugation at 12 000 rpm at 4 °C for 10 min, the supernatant was recovered and was analyzed by HPLC-MS (full-scan analysis). The AUC of the signal of rifabutin, at m/z $[M+H]^+$ = 847, was determined for the rifabutin sample as well as the tested prodrugs. The percentage release of rifabutin was calculated by doing the ratio between the mean AUC signal of the rifabutin released by the prodrugs, and the mean AUC signal of the rifabutin sample.

4.6. Procedure for chemical stability measurement in PBS pH 7.4 or aqueous HCl 26 mM

Experiment was performed in duplicate but were not independent. A solution of 50 mg/mL of the tested compound in extradry DMSO was diluted 100 times with PBS 7.4 or aqueous HCl 0.026M to obtain a solution at 0.5 mg/mL. The samples were vortexed then 50 µL was collected and diluted with 450 µL of CH_3CN (for **11i** and **29**) or MeOH (for **33**). After centrifugation at 12 000 rpm at RT for 10 min, the supernatant was recovered and analyzed. The samples were shaken at 35 rpm with an intelli-mixer over 6 h at RT. 50 µL was collected and the same treatment was performed as for t = 0. The samples were analyzed by UPLC-MS/MS (MRM detection, same parameters than for part 4.2.2 except injection volume of 0.2 µL). The remaining percentage was calculated by doing the ratio between the mean AUC signal of the prodrugs at t = 6 h, and the mean AUC signal of the prodrug at t = 0.

4.7. Procedure for the *in vivo* pharmacokinetic study

Female CD-1 (RjOrl:SWISS) mice (8 weeks old at delivery) were purchased from Janvier Labs, France. The animals were housed in groups in a separate temperature-controlled room (20 to 24°C), with humidity 45 to 65%, and maintained in a 12h light/12h dark cycle. Ventilation was maintained at 15 air changes per hour. Animals were fed ad libitum (Altromin international, 1324TPF) before and during the study. Drinking water was freely available.

All experimental procedures were approved by and conducted in accordance with the regulations of the local Animal Welfare authorities (Landesamt für Gesundheit und Verbraucherschutz, Abteilung Lebensmittel- und Veterinärwesen, Saarbrücken).

Formulations of rifabutin (5 mL/kg, 5mg/kg in 10 % DMSO/90 % NaCl 0.9 % with 26 mM HCl) and prodrugs (5 mL/kg; **11i**, 6.5 mg/kg in NaCl 0.9% with 26 mM HCl, **29**, 6.5 mg/kg in NaCl 0.9% with 26 mM HCl; **34**, 7 mg/kg in PBS, pH 7.4) were administered intravenously in one of the lateral tail vein of female CD-1 mice (9 mice per administered compound). At each of the designated time points (5, 15, 30 min, 1, 2, 4, 8, 12, 24 h), a volume of 100 µL blood was obtained by puncture of the retrobulbar venous plexus into tubes containing Li-Heparin. The samples were stored on ice and subsequently centrifuged at 4500 g for 10 minutes at 4°C. Plasma was harvested and kept at -20°C until processed for bioanalysis. A volume of of 20 µL of each sample was spiked with 2.4 µL of DMSO, then 40 µL of internal standard (griseofulvin, 600 ng/mL in CH_3CN) was added. After centrifugation for 10 min et 8 000 rpm, an aliquot of 50 µL of the supernatant was diluted with 50 µL of fresh water then was analyzed by LC-MS/MS. Release of rifabutin from the samples was dosed, by quantifying the molecule form a calibration curve.
LC-MS/MS informations: analysis were performed on Surveyor MS Plus HPLC system and TSQ Quantum Discovery Max triple quadrupole mass spectrometer equipped with an electrospray (ESI) interface with Kinetex Phenyl-Hexyl, 2.6 µm, 50x2.1 mm (Phenomenex, Germany) analytical column. For a 2. min analysis, the elution was done from 95 % H_2O/5% CH_3CN/0.1% formic acid to 5 % H_2O/95 % CH_3CN/0.1% formic acid over 1.7 min. A flow rate at 600 µL/min was used. Griseofulvin was used as internal standard. Full scan mass spectra were acquired in the positive mode using syringe pump infusion to identify the protonated quasimolecular ions $[M+H]^+$. Auto-tuning was carried out for maximising ion abundance followed by the identification of characteristic fragment ions using a generic parameter set: ion-transfer-capillary temperature 350°C, capillary voltage 3.8 kV, collision gas 0.8 mbar argon, sheath gas, ion sweep gas and auxiliary gas pressure were 20, 2 and 8 (arbitrary units), respectively. Ions with the highest S/N ratio were used to quantify the item in the selected reaction monitoring mode (SRM) and as qualifier, respectively. Monitoring ion was 815.3/755.3 for rifabutin and 215.0 for griseofulvin.

5. Acknowledgment

This research was financially co-funded by European Union under the European Regional Development Fund (ERDF) and by the Hauts De France Regional Council (Contract n°NP0020070).

6. Supplementary data

Supplementary data related to this article can be found at xx.

7. References

[1] Kunin, C. M. Antimicrobial Activity of Rifabutin. *Clin. Infect. Dis. Off. Publ. Infect. Dis. Soc. Am.* **1996**, *22 Suppl 1*, S3-13; discussion S13-14. https://doi.org/10.1093/clinids/22.supplement_1.s3.

[2] Vaara, M. Comparative Activity of Rifabutin and Rifampicin against Gram-Negative Bacteria That Have Damaged or Defective Outer Membranes. *J. Antimicrob. Chemother.* **1993**, *31* (5), 799–801. https://doi.org/10.1093/jac/31.5.799-a.

[3] Gill, S. K.; Garcia, G. A. Rifamycin Inhibition of WT and Rif-Resistant Mycobacterium Tuberculosis and Escherichia Coli RNA Polymerases in Vitro. *Tuberculosis* **2011**, *91* (5), 361–369. https://doi.org/10.1016/j.tube.2011.05.002.

[4] Lin, M.-F.; Lan, C.-Y. Antimicrobial Resistance in Acinetobacter Baumannii: From Bench to Bedside. *World J. Clin. Cases WJCC* **2014**, *2* (12), 787–814. https://doi.org/10.12998/wjcc.v2.i12.787.

[5] World Health Organization, WHO publishes list of bacteria for which new antibiotics are urgently needed. https://www.who.int/news/item/27-02-2017-who-publishes-list-of-bacteria-for-which-new-antibiotics-are-urgently-needed (accessed 13 April 2014).

[6] Janes, J.; Young, M. E.; Chen, E.; Rogers, N. H.; Burgstaller-Muehlbacher, S.; Hughes, L. D.; Love, M. S.; Hull, M. V.; Kuhen, K. L.; Woods, A. K.; Joseph, S. B.; Petrassi, H. M.; McNamara, C. W.; Tremblay, M. S.; Su, A. I.; Schultz, P. G.; Chatterjee, A. K. The ReFRAME Library as a Comprehensive Drug Repurposing Library and Its Application to the Treatment of Cryptosporidiosis. *Proc. Natl. Acad. Sci. U. S. A.* **2018**, *115* (42), 10750–10755. https://doi.org/10.1073/pnas.1810137115.

[7] Luna, B.; Trebosc, V.; Lee, B.; Bakowski, M.; Ulhaq, A.; Yan, J.; Lu, P.; Cheng, J.; Nielsen, T.; Lim, J.; Ketphan, W.; Eoh, H.; McNamara, C.; Skandalis, N.; She, R.; Kemmer, C.; Lociuro, S.; Dale, G. E.; Spellberg, B. A Nutrient-Limited Screen Unmasks Rifabutin Hyperactivity for Extensively Drug-Resistant Acinetobacter Baumannii. *Nat. Microbiol.* **2020**, *5* (9), 1134–1143. https://doi.org/10.1038/s41564-020-0737-6.

[8] Muller, A.; de Winter, B. C. M.; Gitzinger, M.; Kemmer, C.; Lociuro, S.; Pulse, M.; Schellhorn, B.; Trebosc, V.; Weiss, W. J.; Dale, G. E. Pharmacokinetics and pharmacodynamics of BV100 in neutropenic mouse lung infection models. *ECCMID 2021 congress*. **2021**.

[9] Skinner, M. H.; Hsieh, M.; Torseth, J.; Pauloin, D.; Bhatia, G.; Harkonen, S.; Merigan, T. C.; Blaschke, T. F. Pharmacokinetics of Rifabutin. *Antimicrob. Agents Chemother.* **1989**, *33* (8), 1237–1241.

[10] ClinicalTrials.gov, Clinical trial to investigate the safety, tolerability and pharmacokinetics of BV100 in male subjects. https://clinicaltrials.gov/ct2/show/NCT04636983 (accessed 13 April 2014).

[11] ClinicalTrials.gov, Clinical Trial to Investigate the safety, tolerability and pharmacokinetics of BV100 in male subjects. https://clinicaltrials.gov/ct2/show/NCT05087069 (accessed 13 April 2014).

[12] ClinicalTrials.gov, Pharmacokinetics and safety of BV100 administered as single intravenous infusion to subjects with renal impairment. https://clinicaltrials.gov/ct2/show/NCT05086107 (accessed 13 April 2014).

[13] Dietrich, E.; Reddy, R.; Tanaka, K.; Kang, T.; Lafontaine, Y.; Far, A. R. Phosphonated rifamycins and uses thereof for the prevention and treatment of bone and joint infections. *WO2010019511A2*. **2010**.
[14] Dietrich, E.; Reddy, R.; Tanaka, K.; Kang, T.; LaFontaine, Y.; Far, A. R. Phosphonated rifamycins and uses thereof for the prevention and treatment of bone and joint infections. *US20110178001A1*. **2011**.
[15] Figueiredo, R.; Moiteiro, C.; Medeiros, M. A.; Silva, P. A. da; Ramos, D.; Spies, F.; Ribeiro, M. O.; Lourenço, M. C. S.; Júnior, I. N.; Gaspar, M. M.; Cruz, M. E. M.; Curto, M. J. M.; Franzblau, S. G.; Orozco, H.; Aguilar, D.; Hernandez-Pando, R.; Costa, M. C. Synthesis and Evaluation of Rifabutin Analogs against Mycobacterium Avium and H37Rv, MDR and NRP Mycobacterium Tuberculosis. *Bioorg. Med. Chem.* **2009**, *17* (2), 503–511. https://doi.org/10.1016/j.bmc.2008.12.006.
[16] Medeiros, M.; Costa, M.; Figueiredo, R.; Rosa, M.; Curto, M.; Santos, L.; Cruz, M.; Gaspar, M.; Feio, S. Derivatives of Rifabutine Useful as Antimicrobial Agents, January 15, 2004.
[17] Pinheiro, M.; Pereira-Leite, C.; Arêde, M.; Nunes, C.; Caio, J. M.; Moiteiro, C.; Giner-Casares, J. J.; Lúcio, M.; Brezesinski, G.; Camacho, L.; Reis, S. Evaluation of the Structure-Activity Relationship of Rifabutin and Analogs: A Drug-Membrane Study. *Chemphyschem Eur. J. Chem. Phys. Phys. Chem.* **2013**, *14* (12), 2808–2816. https://doi.org/10.1002/cphc.201300262.
[18] Pinheiro, M.; Nunes, C.; Caio, J. M.; Moiteiro, C.; Brezesinski, G.; Reis, S. Interactions of N'-Acetyl-Rifabutin and N'-Butanoyl-Rifabutin with Lipid Bilayers: A Synchrotron X-Ray Study. *Int. J. Pharm.* **2013**, *453* (2), 560–568. https://doi.org/10.1016/j.ijpharm.2013.06.018.
[19] Rose, Y.; Ciblat, S.; Kang, T.; Rafai Far, A.; Dietrich, E.; Lafontaine, Y.; Reddy, R. Phosphonated rifamycins and uses thereof for the prevention and treatment of bone and joint infections. *WO2007096703*. **2007**.
[20] Arora, S. K.; Main, P. Correlation of Structure and Activity in Ansamycins: Molecular Structure of Cyclized Rifamycin SV. *J. Antibiot. (Tokyo)* **1984**, *37* (2), 178–181. https://doi.org/10.7164/antibiotics.37.178.
[21] Haba, K.; Popkov, M.; Shamis, M.; Lerner, R. A.; Barbas III, C. F.; Shabat, D. Single-Triggered Trimeric Prodrugs. *Angew. Chem. Int. Ed.* **2005**, *44* (5), 716–720. https://doi.org/10.1002/anie.200461657.
[22] Amsberry, K. L.; Gerstenberger, A. E.; Borchardt, R. T. Amine Prodrugs Which Utilize Hydroxy Amide Lactonization. II. A Potential Esterase-Sensitive Amide Prodrug. *Pharm. Res.* **1991**, *8* (4), 455–461. https://doi.org/10.1023/a:1015890809507.
[23] Yatzeck, M. M.; Lavis, L. D.; Chao, T.-Y.; Chandran, S. S.; Raines, R. T. A Highly Sensitive Fluorogenic Probe for Cytochrome P450 Activity in Live Cells. *Bioorg. Med. Chem. Lett.* **2008**, *18* (22), 5864–5866. https://doi.org/10.1016/j.bmcl.2008.06.015.
[24] Santos, C.; Mateus, M. L.; dos Santos, A. P.; Moreira, R.; de Oliveira, E.; Gomes, P. Cyclization-Activated Prodrugs. Synthesis, Reactivity and Toxicity of Dipeptide Esters of Paracetamol. *Bioorg. Med. Chem. Lett.* **2005**, *15* (6), 1595–1598. https://doi.org/10.1016/j.bmcl.2005.01.065.
[25] Hamel, A. r.; Hubler, F.; Carrupt, A.; Wenger, R. m.; Mutter, M. Cyclosporin A Prodrugs: Design, Synthesis and Biophysical Properties. *J. Pept. Res.* **2004**, *63* (2), 147–154. https://doi.org/10.1111/j.1399-3011.2003.00111.x.
[26] De, A.; DiMarchi, R. D. Synthesis and Characterization of Ester-Based Prodrugs of Glucagon-like Peptide 1. *Biopolymers* **2010**, *94* (4), 448–456. https://doi.org/10.1002/bip.21418.
[27] Ishii, H.; Koshimizu, T.; Usami, S.; Fujimoto, T. Toxicity of Aspartame and Its Diketopiperazine for Wistar Rats by Dietary Administration for 104 Weeks. *Toxicology* **1981**, *21* (2), 91–94. https://doi.org/10.1016/0300-483X(81)90119-0.

[28] Daisuke, T. Method for selective removal of dibenzofulvene derivative. *US 20100184952 A1*. **2010**.
[29] DiMaio, J.; Jaramillo, J.; Wernic, D.; Grenier, L.; Welchner, E.; Adams, J. Synthesis and Biological Activity of Atrial Natriuretic Factor Analogues: Effect of Modifications to the Disulfide Bridge. *J. Med. Chem.* **1990**, *33* (2), 661–667. https://doi.org/10.1021/jm00164a031.
[30] Li, S.-Z.; Ahmar, M.; Queneau, Y.; Soulère, L. A Convenient Method for Phosphorylation Using Triallyl Phosphite. *Tetrahedron Lett.* **2015**, *56* (32), 4694–4696. https://doi.org/10.1016/j.tetlet.2015.06.030.
[31] Meisenheimer, P.; Walker, J.; Zhou, W. Dual protected pro-coelenterazine substrates, *WO2018049241*. **2018**.
[32] Longcor, J.; Pinchuk, A.; Hoover, R.; Huang, Z. Phospholipid ether conjugates as cancer-targeting drug vehicles. *WO2021050917*. **2021**.
[33] De La Rosa, M. A.; Miller, J. F.; Temelkoff, D.; Velthuisen, E. J.; Naidu, B. N.; Samano, V. Compounds useful in HIV therapy. *WO2020178767*. **2020**..
[34] Huvelle, S.; Alouane, A.; Saux, T. L.; Jullien, L.; Schmidt, F. Syntheses and Kinetic Studies of Cyclisation-Based Self-Immolative Spacers. *Org. Biomol. Chem.* **2017**, *15* (16), 3435–3443. https://doi.org/10.1039/C7OB00121E.
[35] Gavai, A. V.; Han, W.-C.; Fink, B. E.; Guarino, V. R. Prodrugs of 1,4-benzodiazepinone compounds. *WO2014047391*. **2014**.
[36] Zhou, W.; Andrews, C.; Liu, J.; Shultz, J. W.; Valley, M. P.; Cali, J. J.; Hawkins, E. M.; Klaubert, D. H.; Bulleit, R. F.; Wood, K. V. Self-Cleavable Bioluminogenic Luciferin Phosphates as Alkaline Phosphatase Reporters. *ChemBioChem* **2008**, *9* (5), 714–718. https://doi.org/10.1002/cbic.200700644.
[37] Schönberger, M.; Trauner, D. A Photochromic Agonist for μ-Opioid Receptors. *Angew. Chem. Int. Ed.* **2014**, *53* (12), 3264–3267. https://doi.org/10.1002/anie.201309633.
[38] Akagawa, K.; Kudo, K. Construction of an All-Carbon Quaternary Stereocenter by the Peptide-Catalyzed Asymmetric Michael Addition of Nitromethane to β-Disubstituted α,β-Unsaturated Aldehydes. *Angew. Chem. Int. Ed.* **2012**, *51* (51), 12786–12789. https://doi.org/10.1002/anie.201206916.
[39] Ueda, Y.; Mikkilineni, A. B.; Knipe, J. O.; Rose, W. C.; Casazza, A. M.; Vyas, D. M. Novel Water Soluble Phosphate Prodrugs of Taxol® Possessing in Vivo Antitumor Activity. *Bioorg. Med. Chem. Lett.* **1993**, *3* (8), 1761–1766. https://doi.org/10.1016/S0960-894X(00)80058-X.
[40] Bhuket, P. R. N.; Jithavech, P.; Ongpipattanakul, B.; Rojsitthisak, P. Interspecies Differences in Stability Kinetics and Plasma Esterases Involved in Hydrolytic Activation of Curcumin Diethyl Disuccinate, a Prodrug of Curcumin. *RSC Adv.* **2019**, *9* (8), 4626–4634. https://doi.org/10.1039/C8RA08594C.
[41] Nishimuta, H.; Houston, J. B.; Galetin, A. Hepatic, Intestinal, Renal, and Plasma Hydrolysis of Prodrugs in Human, Cynomolgus Monkey, Dog, and Rat: Implications for in Vitro-in Vivo Extrapolation of Clearance of Prodrugs. *Drug Metab. Dispos. Biol. Fate Chem.* **2014**, *42* (9), 1522–1531. https://doi.org/10.1124/dmd.114.057372.
[42] Jin, C.; Wen, S.; Zhang, Q.; Zhu, Q.; Yu, J.; Lu, W. Synthesis and Biological Evaluation of Paclitaxel and Camptothecin Prodrugs on the Basis of 2-Nitroimidazole. *ACS Med. Chem. Lett.* **2017**, *8* (7), 762–765. https://doi.org/10.1021/acsmedchemlett.7b00189.
[43] Cho, S.; Yoon, Y.-R. Understanding the Pharmacokinetics of Prodrug and Metabolite. *Transl. Clin. Pharmacol.* **2018**, *26* (1), 1–5. https://doi.org/10.12793/tcp.2018.26.1.1.
[44] Dale, G. E.; Kemmer, C.; Trebosc, V.; Schellhorn, B.; Gitzinger, M.; Lociuro, S.; Pulse, M.; Weiss, W. J. *In vivo* efficacy of BV100 in mouse models of *Acinetobacter baumannii* infections. *ECCMID 2021 congress*. **2021**.

[45] Kraljić, K.; Jelić, D.; Žiher, D.; Cvrtila, A.; Dragojević, S.; Sinković, V.; Mesić, M.Benzoxaboroles—Novel Autotaxin Inhibitors. *Molecules* **2019**, *24* (19), 3419. https://doi.org/10.3390/molecules24193419.